Rare Decay Modes of the η Meson*

BING-LIN YOUNG
Department of Physics, Indiana University, Bloomington, Indiana
(Received 6 April 1967)

The rare decay modes of the η meson are considered. Since in these decays the electromagnetic interaction for the leptons is well known, this work is concentrated on the strong interactions acting at the $\eta\gamma\gamma$ vertex. A model for the form factor of this vertex function is constructed. In this model the low-energy and the high-energy behavior of the form factor are separately considered. The Bjorken limit is applied to determine the asymptotic behavior of the form factor. Predictions on the branching ratios of both the Dalitz pair and the direct decay modes are given as functions of the various parameters involved. Further experiments are needed to determine these parameters. A discussion of the model is also presented.

I. INTRODUCTION

WE shall concern ourselves with the following decay modes of the η meson:

$$\eta \to \gamma+\mu^+ +\mu^-, \tag{I1}$$

$$\eta \to \gamma+e^+ +e^-, \tag{I2}$$

$$\eta \to \mu^+ +\mu^-, \tag{I3}$$

$$\eta \to e^+ +e^-. \tag{I4}$$

Processes (I1), (I2), and (I3), and (I4) are known, respectively, as the Dalitz pair[1] and direct decay modes. The processes corresponding to (I2), (I4) for π^0 have been considered in several recent papers[2-4]; processes (I1)–(I3) have also been considered.[5]

To lowest order in the electromagnetic interaction, these processes, and the corresponding processes for π^0 decay are related to the $\eta\gamma\gamma$ and $\pi^0\gamma\gamma$ vertex functions. These vertex functions are expressible in terms of the two form factors $\Gamma_\eta(k_1^2,k_2^2)$ and $\Gamma_{\pi^0}(k_1^2,k_2^2)$, where k_1^2 and k_2^2 are the photon masses. These form factors contain to all orders the strong interactions that are responsible for the transition η, $\pi^0 \to 2\gamma$. We use the properties of $\Gamma_{\eta,\pi^0}(k_1^2,k_2^2)$, which may be inferred by knowing the branching ratios of the above processes with η, $\pi^0 \to 2\gamma$, and the lepton-pair distributions of the Dalitz-pair decays, to investigate these strong interactions.

Let us sketch how each of these processes relates to the form factors and what we expect to learn from them. Since past work treats π^0,[1-4] we shall start with this case.

The relation between the Dalitz-pair decay and the $\pi^0\gamma\gamma$ vertex can be seen from the following transition:

$$\pi^0 \to \gamma+\gamma \searrow e^+ +e^-.$$

Its branching ratio to $\pi^0 \to 2\gamma$ is the order of 2α, and has been checked experimentally. The electron-pair distribution provides a way to study the form factor $\Gamma_{\pi^0}(0,k^2)$, where k^2 is the virtual photon mass squared.

Use of the vector-meson-dominance model, together with $SU(3)$ symmetry, enables us to evaluate this form factor and thus gives a definite prediction for the distribution of the outgoing leptons. We can therefore use this prediction to obtain a check on the combination of the vector-meson-dominance model and $SU(3)$ symmetry.

The direct decay process relates to the form factor in the following way [see Fig. 1(c)]:

$$\pi^0 \to \gamma+\gamma \to e^+ +e^-.$$

To obtain the amplitude for direct decay, an integration over all the possible virtual photon momenta has to be performed. The result is, however, divergent unless the form factor provides a damping effect when the virtual photon momenta become large. This particular aspect of the direct decay implies that $\Gamma_{\pi^0}(k_1^2,k_2^2)$ cannot be constant. Unfortunately, the branching ratio $\Gamma_{\pi^0\to e^+ +e^-}/\Gamma_{\pi^0\to 2\gamma}$ is about $2\alpha m_e^2/m_{\pi^0}^2 \sim 10^{-8}$ (Refs. 2, 4) which means that the decay will be very hard to observe.

A parallel situation holds for η. Nevertheless, because of its higher mass, the μ-pair channels are open and provide useful applications.

The branching ratios of the Dalitz-pair decays to the decay $\eta \to 2\gamma$ are also of order α. Now $0<k^2\leqslant m_\eta^2$; since $m_\eta^2 \approx 16 m_{\pi^0}^2$, $\Gamma_\eta(0,k^2)$ can be probed to a larger extent than $\Gamma_{\pi^0}(0,k^2)$. Another interesting feature of these Dalitz-pair decay modes is to provide a possible test of the difference between e electrodynamics and μ electrodynamics for a timelike low-energy photon.[5]

For the direct decays of η, we estimate the following branching ratios:

$$\Gamma_{\eta\to e^+e^-}/\Gamma_{\eta\to 2\gamma} \sim 2\alpha^2 m_e^2/m_\eta^2 \sim 10^{-9},$$

$$\Gamma_{\eta\to \mu^+\mu^-}/\Gamma_{\eta\to 2\gamma} \sim 2\alpha^2 m_\mu^2/m_\eta^2 \sim 10^{-5}.$$

The e-pair process is again too small to be interesting. The μ-pair process is expected to be observable. As will become clear later, its sensitivity to the structure of $\Gamma_\eta(k_1^2,k_2^2)$ enables us to make observations and predictions which are hopefully to be checked by future experiments.

* This work is based on part of a thesis submitted by the author to the University of Minnesota in partial fulfillment of the requirements of the Ph.D. degree. Supported by the U. S. Atomic Energy Commission.

[1] R. H. Dalitz, Proc. Phys. Soc. (London) **A64**, 667 (1951).
[2] S. D. Drell, Nuovo Cimento **11**, 693 (1959).
[3] S. M. Berman and D. A. Geffen, Nuovo Cimento **18**, 1192 (1960).
[4] How-sen Wang, Phys. Rev. **121**, 289 (1961).
[5] D. A. Geffen and Bing-lin Young, Phys. Rev. Letters **15**, 316 (1965).

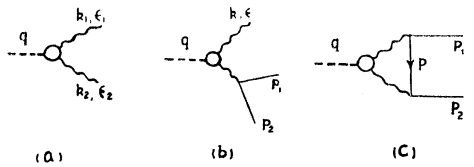

FIG. 1. Feynman diagrams of the decays: (a) $\eta \to 2\gamma$, (b) $\eta \to l^+ + l^- + \gamma$, (c) $\eta \to l^+ + l^-$. Only first order in the electromagnetic interaction is considered.

In the previous work[2,3] the high-energy behavior of $\Gamma_{\pi^0}(k_1^2, k_2^2)$ has not been investigated, but instead *ad hoc* cutoff-type functions were assumed in the calculations. There are difficulties associated with these form factors. For instance in Ref. 3, the assumed form factor does not satisfy the analytic property [Eq. (2.2), Ref. 3] derived from the general spectral condition.[6] A modification of results of Refs. 2 and 3 to be applicable to the case of η has been carried out in Ref. 5, and the numerical results indicate that the model of Ref. 3 is very insensitive to the cutoff mass, while that of Ref. 2 depends strongly on the cutoff masses.

In this paper we shall present a model for the vertex function $\Gamma_\eta(k_1^2, k_2^2)$. The attractive model of vector dominance of the low-energy behavior of the electromagnetic interaction of hadrons is applied. In the language of dispersion relations, this is equivalent to the statement that at small virtual-photon masses only the vector-meson contributions have to be considered in the intermediate states. The question of subtractions is guided by the following consideration: Since an unsubstracted dispersion relation (by means of vector-dominance model) does not predict the π^0 lifetime correctly, the subtractions are in order. In our treatment, one subtraction will be taken. For the high-energy behavior we construct a model which is guided by the approximation that at high energies the ηVV interaction ($V \equiv$ a vector particle) can be mediated through nucleon intermediate states. The asymptotic behavior of the form factor is subjected to the condition of the Bjorken limit.[7] The resultant form factor can be shown to satisfy the analyticity properties derived from the general spectral condition. In view of the lack of a reliable theory for treating high-energy behavior of form factors, hopefully the present model incorporating the Bjorken limit will provide some understanding of the high-energy properties of the frorm factor.

In Sec. II we list the formulas for the differential cross sections of the Dalitz-pair (DP) and direct (D) decays with respect to the 2γ decay mode. Two important properties of the vertex function are mentioned in Sec. III. Section IV is devoted to the construction of a model of $\Gamma_\eta(k_1^2, k_2^2)$. Predictions on the decay branching ratios and the Dalitz-pair distributions are presented in Sec. V. In Sec. VI we discuss the general features of the model.

[6] I am indebted to Professor Geffen for pointing this out to me.
[7] J. D. Bjorken, Phys. Rev. **148**, 1467 (1966).

II. FORMULAS OF THE DECAY BRANCHING RATIOS

To lowest order in the electromagnetic interaction, the decay amplitude of the processes $\eta \to 2\gamma$, $\eta \to l^+ + l^- + \gamma$, and $\eta \to l^+ + l^-$ can be written, respectively, as[8]

$$T_2 = \epsilon_1^\mu \epsilon_2^\nu \varepsilon_{\mu\nu\lambda\tau} \frac{k_1^\lambda k_2^\tau}{m_\pi} \Gamma_\eta(0,0), \tag{II1}$$

$$T_3 = -ie\bar{u}(p_2)\gamma^\mu v(p_1) \frac{1}{(q-k)^2} \epsilon^\nu \varepsilon_{\mu\nu\lambda\tau} \frac{k^\lambda q^\tau}{m_\pi} \times \Gamma_\eta(0, (q-k)^2), \tag{II2}$$

$$T_4 = -\frac{ie^2}{(2\pi)^4} \bar{u}_\lambda(p_2)\gamma_{\lambda\lambda'\nu}\gamma_{\tau'\tau}{}^\mu v_\tau(p_1) \varepsilon_{\mu\nu\sigma\rho} \frac{1}{m_{\pi^0}} \int d^4p \times \frac{(m_l + \not{p})^{\lambda'\tau'}(p_1+p)^\sigma (p_2-p)^\rho}{(p^2 - m_l^2 + i\epsilon)[(p_1+p)^2 + i\epsilon][(p_2-p)^2 + i\epsilon]} \times \Gamma_\eta((p_1+p)^2, (p_2-p)^2), \tag{II3}$$

where, with $k_1 + k_2 = q$, the $\eta\gamma\gamma$ form factor $\Gamma_\eta(k_1^2, k_2^2)$ is defined by

$$\Gamma_{\mu\nu}(k_1,k_2) \equiv \varepsilon_{\mu\nu\lambda\tau} \frac{k_1^\lambda k_2^\tau}{m_\pi} \Gamma_\eta(k_1^2, k_2^2) = i \int d^4x \, e^{i(k_1 - k_2)\cdot x/2} \times \langle 0 | T\{J_\mu(x/2), J_\nu(-x/2)\} | q \rangle. \tag{II4}$$

The Feynman diagrams of the above processes to the given order in the electromagnetic interaction are illustrated in the diagrams of Fig. 1. In the above expressions we use q to denote the four-momentum of the η and ϵ to denote the outgoing photon polarization. Also k_1, k_2, k, p_1, and p_2 are the momenta of the various outgoing particles in the appropriate processes. The details can be read from Fig. 1.

Let us denote the corresponding decay rates of the above processes by R_2, R_3, and R_4, respectively. We have the decay branching ratios:

$$r_{\mathrm{DP}} \equiv \frac{R_3}{R_2} = \int_{4\xi_l^2}^1 dx \frac{dr_{\mathrm{DP}}}{dx}, \tag{II5}$$

$$\frac{dr_{\mathrm{DP}}}{dx} \equiv \frac{2\alpha}{3\pi} \left| \frac{\Gamma_\eta(0, m_\eta^2 x)}{\Gamma_\eta(0,0)} \right| \frac{1}{x} (1-x)^3 \times \left(1 - \frac{4\xi_l^2}{x}\right)^{1/2} \left(1 + \frac{2\xi_l^2}{x}\right), \tag{II6}$$

$$r_{\mathrm{D}} \equiv \frac{R_4}{R_2} = \frac{1}{2} \left(\frac{\alpha}{\pi}\right)^2 (1 - 4\xi_l^2) \left| \frac{1}{\Gamma_\eta(0,0)} \right|^2 \times |3A + (1 - 4\xi_l^2)B|^2, \tag{II7}$$

[8] We use a positive metric, i.e., $a \cdot b = a_0 b_0 - \mathbf{a} \cdot \mathbf{b}$, and natural units $\hbar = c = 1$.

where $\xi_l=m_l/m_\eta$. Here A and B are invariant scalar functions and are defined by means of the following expression:

$$\int d^4p \frac{p^\lambda p^\tau \Gamma_\eta((q-p)^2, p^2)}{[(p_2-p)^2-m_l^2+i\epsilon](p^2+i\epsilon)[(q-p)^2+i\epsilon]} = \frac{i\pi}{2}\left(Ag^{\lambda\tau}-4\frac{p^\lambda p^\tau}{m_\eta^2}B\right). \quad \text{(II8)}$$

The above formulas hold also for π^0 if we replace Γ_η by Γ_{π^0} and m_η by m_{π^0}. In this case, of course we have e-pair processes only.

III. PROPERTIES OF THE FORM FACTOR

We state some of the properties of $\Gamma_\eta(k_1^2,k_2^2)$ that will be useful in later discussions.

A. Symmetry Property and the Absorptive Part of the Form Factor

From the definition of $\Gamma_\eta(k_1^2,k_2^2)$ (II4), it is easy to show that the form factor possesses the following symmetry property:

$$\Gamma_\eta(k_1^2,k_2^2)=\Gamma_\eta(k_2^2,k_1^2). \quad \text{(III1)}$$

The absorptive part of $\Gamma_\eta(k_1^2,k_2^2)$ can be obtained by applying PT invariance to (II4).[9] We report only the result:

$$\varepsilon_{\mu\nu\lambda\tau}\frac{k_1^\lambda k_2^\tau}{m_\pi}\mathrm{Im}\Gamma_\eta(k_1^2,k_2^2)=\frac{1}{2}\int d^4x\, e^{i(k_1-k_2)\cdot x/2} \times\langle 0|\{J_\mu(x/2), J_\nu(-x/2)\}|q\rangle. \quad \text{(III2)}$$

B. Asymptotic Behavior of $\Gamma_\eta(k_1^2,k_2^2)$

The asymptotic behavior of the form factor is[10]

$$\Gamma_\eta(k^2,(q-k)^2)\xrightarrow[|k_0|\to\infty]{}-\frac{e^2}{k_0^2}\frac{2C_{\pi^0}m_{\pi^0}}{3\sqrt{3}}. \quad \text{(III3)}$$

The above result is obtained by means of the method discussed in Bjorken's recent work on current algebra.[7] The derivation of (III3) will be given in Appendix A. We shall call (III3) the Bjorken limit and shall denote the coefficient of the Bjorken limit as

$$C_{\mathrm{BL}}=-2e^2C_{\pi^0}/3\sqrt{3}. \quad \text{(III4)}$$

[9] From the analysis of J. Bernstein, G. Finberg, and T. D. Lee [Phys. Rev. **139**, B1650 (1965)], it can be shown that (II2) holds even without the assumption of T invariance for the electromagnetic interaction of hadrons.

[10] We like to point out that the $1/k_0^2$ asymptotic behavior of $\Gamma_\eta(k_1^2,k_2^2)$ can be obtained by other methods. For example, in the Dyson representation [F. Dyson, Phys. Rev. **110**, 1460 (1958)], if a suitable convergence condition on the spectral function is assumed, this behavior is obtainable. However, the coefficient (III4) cannot be obtained in the Dyson representation.

IV. EVALUATION OF THE FORM FACTOR

In this section we shall construct a model for the form factor. The method applies also to the corresponding π^0 form factor $\Gamma_{\pi^0}(k_1^2,k_2^2)$.

The k_1^2, k_2^2 dependence of the form factor in general can be separated into different energy regions. Each energy region is characterized by the intermediate states dominating the form factor. For example, at low energies only the low-lying states are important; this has been shown to be true for the pion and nucleon form factors. As the energy becomes higher and higher, more and more intermediate states become accessible to the process under consideration. It is not unreasonable to contemplate that at sufficiently high energies the contribution of the relatively low-lying states become less important, and the process considered is characterized by high-mass intermediate states.

With such preliminary understanding we shall make a few assumptions which form an integral part of our investigation and are crucial to the construction of the model.

(a) The form factor $\Gamma_\eta(k_1^2,k_2^2)$ can be factored into two parts which give the low-energy and high-energy contributions:

$$\Gamma_\eta(k_1^2,k_2^2)=H(k_1^2,k_2^2)L(k_1^2,k_2^2), \quad H(0,0)=1, \text{ i.e., } L(0,0)=\Gamma_\eta(0,0), \quad \text{(IV1)}$$

where H and L are, respectively, the high-energy and low-energy functions which dominate at the respective energy regions.

(b) The low-energy function $L(k_1^2,k_2^2)$ is dominated by the vector-meson intermediate states (ρ^0, ω, and φ) and satisfies a once-subtracted dispersion relation in k_1^2, when k_2^2 is fixed, and vice versa. The quantity $L(k_1^2,k_2^2)$ has a cut in each of the variables k_1^2 and k_2^2 from $4m_\pi{}^2$ to M^2, where $M\geqslant 2M_N$ (M_N is the nucleon mass). This particular choice of M comes from the consideration of the analyticity property of the high-energy function. We also assume

$$\lim_{|k_0|\to\infty} L(k^2,(q-k)^2)=\mathrm{const}\equiv L_\infty. \quad \text{(IV2)}$$

(c) The high-energy function $H(k_1^2,k_2^2)$ represents contributions of the high-mass and multiple-particle intermediate states, and has a cut from M^2 to ∞ in one of its arguments when the other one is fixed. Equations

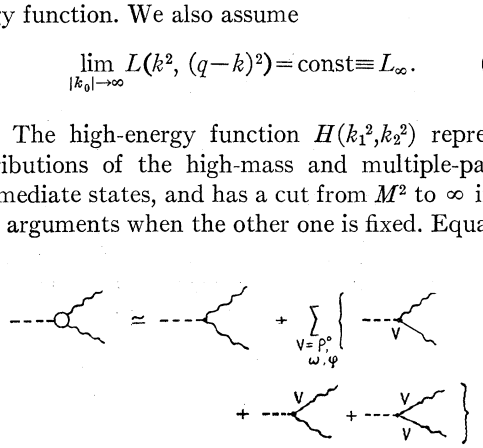

FIG. 2. Vector-meson-dominance model for the low-energy function of the $\eta\gamma\gamma$ form factor.

(III3) and (IV2) imply

$$\lim_{|k_0|\to\infty} H(k^2,(q-k)^2)=\text{const}/k_0^2\equiv H_\infty/k_0^2. \quad \text{(IV3)}$$

(d) In analogy to (III1) we take

$$L(k_1^2,k_2^2)=L(k_2^2,k_1^2), \quad H(k_1^2,k_2^2)=H(k_2^2,k_1^2).$$

A. The Low-Energy Function—Vector-Meson-Dominance Model

From assumption (b) we can write

$$L(k_1^2,k_2^2)=L(k_1^2,0)+\frac{k_2^2}{\pi}\int_{4m_\pi^2}^{M^2}dx\,\frac{\mathrm{Im}L(k_1^2,x)}{x(x-k_2^2)} \quad \text{(IV4)}$$

and

$$L(k_1^2,0)=L(0,0)+\frac{k_1^2}{\pi}\int_{4m_\pi^2}^{M^2}dx\,\frac{\mathrm{Im}L(x,0)}{x(x-k_1^2)}. \quad \text{(IV5)}$$

Since for $4m_\pi^2\leqslant k_i^2\leqslant M^2$,

$$\mathrm{Im}L(k_1^2,k_2^2)=\mathrm{Im}\Gamma_\eta(k_1^2,k_2^2)/H(k_1^2,k_2^2),$$

then $\mathrm{Im}L(k_1^2,k_2^2)$ can be evaluated by means of (III2). Only the vector mesons ρ^0, ω, and φ are considered in the intermediate states. The evaluation of (IV5) is standard. To evaluate (IV4) we have to express the $V\eta\gamma$ vertex function ($V\equiv\rho^0,\omega,\varphi$) as a function of k_1^2. This vertex function can be calculated, using a once-subtracted dispersion relation,[11] by means of vector-meson-dominance model in terms of the phenomenological coupling constants of the $V\eta\gamma$ and $VV'\eta$ interactions. The final result is

$$L(k_1^2,k_2^2)$$

$$=\Gamma_\eta(0,0)+\sum_{i=\rho^0,\omega,\varphi}\left\{\frac{\lambda_i f_i k_1^2}{(m_i^2-k_1^2)H_i}+\frac{\lambda_i f_i k_2^2}{(m_i^2-k_2^2)H_i}\right\}$$

$$+\sum_{i,j=\rho^0,\omega,\varphi}\frac{\lambda_i\lambda_j g_{ij}k_1^2k_2^2}{(m_i^2-k_1^2)(m_j^2-k_2^2)H_{ij}}, \quad \text{(IV6)}$$

where $H_i=H(m_i^2,0)$, $H_{ij}=H(m_i^2,m_j^2)$, and λ_i are the dimensionless phenomenological coupling constants of V_i and γ, f_i that of $V_i\eta\gamma$, and g_{ij} that of $V_iV_j\eta$, where $i,j=\rho^0,\omega,\varphi$. Equation (IV6) is expressed diagramatically in Fig. 2.

Although we have obtained an explicit expression for the low-energy function, its usefulness depends on our knowledge of the various coupling constants f_i and g_{ij}. At the present time, since the experimental situation does not allow us to evaluate them phenomenologically, we must resort to a model calculation. Using the methods of the algebra of currents we have obtained relations between the coupling constants of the $V\eta\gamma$ and $VV\eta$ interactions, respectively.[12] The results are that to the first order in the symmetry-breaking effect, the relations so obtained are identical to those obtained from the Lagrangian approach of exact $SU(3)$ symmetry.

We use the popular choice of the ω-φ mixing angle $\sin\theta=1/\sqrt{3}$,[13] and assume $f_{\varphi\pi\gamma}\simeq 0$ and $g_{\rho\varphi\pi}\simeq 0$,[14] then we can calculate all the relevant coupling constants as follows[12,15]:

$$\lambda_\rho=e/\gamma_\rho, \quad \lambda_\omega=-(e/3\gamma_\rho)m_\rho^2/m_\omega^2, \quad \lambda_\varphi=(e/3\gamma_\rho)m_\rho^2/m_\varphi^2, \quad \text{(IV7)}$$

$$f_{\rho\eta\gamma}\simeq-(1/\sqrt{3})f_{\omega\pi\gamma}, \quad f_{\omega\eta\gamma}\simeq(1/3\sqrt{3})f_{\omega\pi\gamma},$$
$$f_{\varphi\eta\gamma}\simeq(2\sqrt{2}/3\sqrt{3})f_{\omega\pi\gamma}, \quad g_{\rho\rho\eta}\simeq(-1/\sqrt{3})g_{\rho\omega\pi},$$
$$g_{\omega\omega\eta}\simeq(1/3\sqrt{3})g_{\rho\omega\pi}, \quad g_{\varphi\varphi\eta}\simeq(2/\sqrt{3})g_{\rho\omega\pi}, \quad g_{\omega\varphi\eta}\simeq 0, \quad \text{(IV8)}$$

where γ_ρ is the $\rho\pi\pi$ coupling constant and is calculated from the decay $\rho\to 2\pi$. The constant $f_{\omega\pi\gamma}$ can be calculated from $\omega\to\pi+\gamma$, and $g_{\rho\omega\pi}$ from[16]

$$\omega\to\pi+\rho\searrow 2\pi.$$

Using the following pieces of information[17]:

$$\Gamma_{\omega\to\pi+\gamma}\simeq 1.3\text{ MeV}, \quad \Gamma_{\omega\to 3\pi}\simeq 10.6\text{ MeV}, \quad \Gamma_{\rho\to 2\pi}\simeq 120\text{ MeV},$$

we get[18]

$$f_{\omega\pi\gamma}^2/4\pi\simeq 0.186\alpha, \quad g_{\rho\omega\pi}^2/4\pi\simeq 0.5, \quad \gamma_\rho^2/4\pi\simeq 2.4. \quad \text{(IV9)}$$

The form factor at zero photon masses, $\Gamma_\eta(0,0)$, can be determined from the decay width $\eta\to 2\gamma$. In fact, because of the experimental uncertainty, $\Gamma_\eta(0,0)$ is determined from $\Gamma_{\pi^0}(0,0)$ by $\mathfrak{U}$-spin conservation,

---

[11] We cite two reasons that we are in favor of a subtracted dispersion relation in evaluating the $V\eta\gamma$ form factor by means of the vector-meson-dominance model. The first is that a gauge-invariant coupling of V-γ as we have used makes this form factor tend to a constant when the virtual-photon mass becomes large. The second is that an unsubtracted dispersion gives $f_{\rho\pi\gamma}=-(e/3\gamma_\rho)g_{\rho\omega\pi}$. When we incorporate this relation with a recent work of A. Donnachie and G. Shaw [Ann. Phys. (N.Y.) **37**, 333 (1966)] who found $f_{\rho\pi\gamma}\simeq 0$ in fitting the experimental data of pion photoproduction, we obtain $g_{\rho\omega\pi}\simeq 0$ which is a disturbing result and makes the decay $\omega\to 3\pi$ difficult to understand from the viewpoint of the present theoretical framework.

[12] Bing-lin Young, Ph.D. thesis, University of Minnesota, 1966 (unpublished).

[13] The value of the ω-φ mixing angle is not settled yet. The value we used is supported by both the mass formula and the algebra-of-currents calculations. For the latter we refer to M. P. Khanna and A. Vaidya, Trieste report, 1966 (unpublished).

[14] $g_{\rho\omega\pi}\simeq 0$ is supported by experiment. Although we expect $g_{\rho\varphi\pi}^2/4\pi$ to be the order of unity, phenomenologically we find $g_{\rho\varphi\pi}^2/4\pi\simeq\alpha^2$. Since we also expect $f_{\varphi\pi\gamma}\simeq(e/\gamma_\rho)g_{\rho\omega\pi}$ then $f_{\varphi\pi\gamma}^2/4\pi\simeq\alpha^3$, but theoretically we expect $f_{\varphi\pi\gamma}^2/4\pi$ to be of the order of α.

[15] Relations (IV7) agree with what were used by Y. S. Kim *et al.* [Phys. Rev. **135**, B1076 (1965)] but do not agree with those obtained by taking into account the mass-breaking effect. See for example Ref. 5.

[16] M. Gell-Mann, D. Sharp, and W. G. Wagner, Phys. Rev. Letters **8**, 261 (1962).

[17] A. H. Rosenfeld *et al.*, Rev. Mod. Phys. **37**, 633 (1965).

[18] A calculation of all the radiative decay rates of the vector mesons by means of (IV8) and (IV9) has been carried out in Ref. 12. The results are consistent with the existing experimental data.

i.e., $\Gamma_\eta(0,0)=\Gamma_{\pi^0}(0,0)/\sqrt{3}$. Taking $\tau_{\pi^0}\simeq 1.78\times10^{-16}$ sec,[19] we get

$$\Gamma_\eta(0,0)\simeq 1.38\times10^{-3}.$$

B. The High-Energy Function—Cutoff Function

Since there is no reliable theory for treating the high-energy function, the best we can do is to construct a reasonable model for it. We may imagine that at high energies each of the ηVV couplings is mediated by some high-mass intermediate states. The simplest picture is that each single ηVV vertex is replaced by a triangular graph. If we look at this type of process in perturbation theory, considering only Fermi coupling, we are led to a high-energy function of the following form[20]:

$$H(k_1^2,k_2^2)=\int_{\Lambda_1}^{\infty} d\Lambda\,\rho(\Lambda)\frac{\Lambda^2}{(\Lambda-k_1^2)(\Lambda-k_2^2)}, \quad \text{(IV10)}$$

where $\Lambda_1\gtrsim 4M_N^2$ (M_N is the nucleon mass). Here $\rho(\Lambda)$ is the so-called spectral function, and represents all the high-mass contributions to the ηVV, $\eta V\gamma$, and $\eta\gamma\gamma$ vertices. By (IV1) $\rho(\Lambda)$ satisfies the normalization condition:

$$\int_{\Lambda_1}^{\infty}\rho(\Lambda)d\Lambda=1. \quad \text{(IV11)}$$

In the nucleon intermediate-state approximation, $\rho(\Lambda)$ has the form

$$\rho(\Lambda)=(\Lambda_1/\Lambda^2)\theta(\Lambda-\Lambda_1), \quad \text{(IV12)}$$

where $\Lambda_1=4M_N^2$.

If we take this approximation seriously we have to include the contribution of all the other members of the baryon octet. Furthermore, if we argue that all members of the baryon octet contribute with equal probability and that only their average contribution is relevant[21] then the spectral function is still in the form of (IV12), but Λ_1 has to be replaced by the average mass of the baryon octet: $\Lambda_1=4\times(1150)^2$ MeV^2. We shall call this model of the spectral function the baryon model.

We shall show in Appendix B that the Bjorken limit (III3) and the normalization condition (IV11) require the spectral function to possess the following asymptotic behavior:

$$\lim_{\Lambda\to\infty}\rho(\Lambda)\to \text{const}/\Lambda^2. \quad \text{(IV13)}$$

Incidentally $\rho(\Lambda)$ defined by (IV12) has the correct asymptotic form; however, as we shall point out later, it does not possess the correct coefficient.

By inserting all the known numerical factors in (IV6) and (III4), we obtain

$$L_\infty=\Gamma_\eta(0,0)+\text{sgn}(f_{\omega\pi\gamma}/\gamma_\rho)\,19.3\times10^{-3}\frac{[f_{\omega\pi\gamma}^2/4\pi]^{1/2}}{H_\rho}\times(1+0.11H_\rho/H_\omega-0.25H_\rho/H_\varphi)-\text{sgn}(g_{\rho\omega\pi})\times6.2\times10^{-3}\frac{[g_{\rho\omega\pi}^2/4\pi]^{1/2}}{H_{\rho\rho}}\times(1+0.1H_{\rho\rho}/H_{\omega\omega}-0.14H_{\rho\rho}/H_{\varphi\varphi}), \quad \text{(IV14)}$$

$$C_{\text{BL}}=\text{sgn}(g_{NN\pi})1.3\times10^{-3}m_\eta^2.$$

Recall $H_\rho=H(m_\rho^2,0)$, $H_{\rho\rho}=H(m_\rho^2,m_\rho^2)$, etc. Combining the above equations with (IV3), we have

$$H_\infty L_\infty/m_\eta^2\simeq\text{sgn}(g_{NN\pi})1.3\times10^{-3}. \quad \text{(IV15)}$$

Since with a reasonable choice of $\rho(\Lambda)$, H_ρ, etc. are all of order unity, (IV14) shows that L_∞ is dominated by the term proportional to $f_{\omega\pi\gamma}$ and its sign is determined by the sign of $f_{\omega\pi\gamma}/\gamma_\rho$. Because of the relatively small value of C_{BL} it is easy to see that (IV15) can be satisfied only when $|H_\infty/m_\eta^2|<1$. For the baryon model, we have $H_\infty/m_\eta^2\simeq-17.6$. Hence the Bjorken limit cannot be satisfied.

An immediate generalization of (IV12) is

$$\rho(\Lambda)=\sum_{i=0}^{n}\left(\frac{\beta_i\Lambda_i}{\Lambda^2}\right)\theta(\Lambda-\Lambda_i). \quad \text{(IV16)}$$

This model is suggested by the consideration that at high energies, in addition to the baryon octet, there are other groups of particles, each with an effective mass $\Lambda_i^{1/2}/2$, which contribute to the ηVV vertices as the baryon octet does. The importance of the contribution of each of the groups of particles is measured by the dimensionless quantities β_i, $i=0, 1, \cdots n$ which satisfy the relations

$$\sum_{i=0}^{n}\beta_i=1, \quad H_\infty/m_\eta^2=-\sum_{i=0}^{n}\beta_i\Lambda_i/m_\eta^2. \quad \text{(IV17)}$$

For $n=1$, if Λ_0 and Λ_1 are known, β_0 and β_1 are determined by means of (IV15) and (IV17). In general there are $n-1$ parameters in the model (IV16) even if all the masses are given.

In the numerical calculations we shall use the following four models for $\rho(\Lambda)$:

baryon model $\rho(\Lambda)=(\Lambda_1/\Lambda^2)\theta(\Lambda-\Lambda_1)$,

δ-function model $\rho(\Lambda)=\delta(\Lambda-\Lambda_1)$,

single-pole model $\rho(\Lambda)=[(\Lambda_1+C)/(\Lambda+C)^2]\theta(\Lambda-\Lambda_1)$,

dipole model $\rho(\Lambda)=(\beta\Lambda_0/\Lambda^2)\theta(\Lambda-\Lambda_0)+[(1-\beta)\Lambda_1/\Lambda^2]\theta(\Lambda-\Lambda_1)$,

where $\Lambda_1=4\times(1150)^2$ MeV^2.

We should like to remark that the baryon model and the δ-function model do not satisfy the Bjorken limit, while the simple-pole model and the dipole model do.

[19] See Ref. 17. Recently [*Proceedings of the XIIIth International Conference on High-Energy Physics* (University of California Press, Berkeley, California, 1967)] a smaller value for the π^0 lifetime is reported.

[20] For details we refer to Ref. 12.

[21] G. Barton and B. G. Smith, Nuovo Cimento **36**, 436 (1965).

Their predictions on the direct decay branching ratios will enable us to investigate the plausibility of the Bjorken limit.

The parameters β and C in the above spectral functions are determined by substituting the corresponding spectral function into (IV10) and solving Eq. (IV15). Because of the smallness of the Bjorken limit, β and C are not sensitive to the variation of the vector coupling constants and $\Gamma_\eta(0,0)$. However, they vary considerably with respect to changes in Λ_1. For example, the average values of β are 2.8, 1.6, 1.1, and 1.02 for $\Lambda_1/m_\eta^2 = 27.6$, 46.9, 311, and 761, respectively, and the average values of C are -17.3, -46, -187, and -1173 for $\Lambda_1/m_\eta^2 = 17.6$, 46.9, 188, and 1174, respectively. The result that $C \simeq -\Lambda_1$ again reflects the smallness of the Bjorken limit.

V. CALCULATION

We can now calculate r_{DP}, dr_{DP}/dx, and r_{D} by using the form factor derived in the last section. Because of the uncertainties in the experimental information, we have used the following input data:

$$\Gamma_\eta(0,0) \simeq 1.38\times10^{-3} \text{ and } 1.80\times10^{-3},$$
$$f_{\omega\pi\gamma}^2/4\pi \simeq 0.186\alpha \text{ and } 0.14\alpha,$$
$$g_{\rho\omega\pi}/4\pi \simeq 0.5 \text{ and } 0.3.$$

The difference in the values of $f_{\omega\pi\gamma}^2/4\pi$ and $g_{\rho\omega\pi}^2/4\pi$ listed above correspond to a 30% modification in the over-all effects of the vector-meson contributions. The V-γ couplings we used in (IV8) introduce a violation of the U-spin conservation.[22] The values of $\Gamma_\eta(0,0)$ listed above also give a 30% violation in the U-spin conservation.

A. The Dalitz-Pair Decays

The form factor of the Dalitz-pair decay modes is obtained by putting one of the arguments of $\Gamma_\eta(k_1^2,k_2^2)$ at zero, i.e., $\Gamma_\eta(0, (q-k)^2)$, where $q-k$ is the sum of the four-momenta of the lepton pair. Let us write $(q-k)^2 = (p_1+p_2)^2 = m_\eta^2 x$, since $0 < (q-k)^2 \leqslant m_\eta^2$, $4m_l^2/m_\eta^2 \leqslant x \leqslant 1$, we can expand $\Gamma_\eta(0,m_\eta^2 x)$ in powers of x. For small x we can write

$$\Gamma_\eta(0,m_\eta^2 x) \simeq \Gamma_\eta(0,0)(1+a_\eta x).$$

From the work of the last section, we have

$$a_\eta = -\mathrm{sgn}(f_{\omega\pi\gamma}/[\gamma_\rho \Gamma_\eta(0,0)]) 5\times10^{-3} \frac{(f_{\omega\pi\gamma}^2/4\pi)^{1/2}}{H_\rho |\Gamma_\eta(0,0)|}$$
$$\times\left(1+\frac{0.1H_\rho}{H_\omega}-\frac{0.14H_\rho}{H_\varphi}\right)+\int_{\Lambda_1}^{\infty} d\Lambda\, \rho(\Lambda) m_\rho^2/\Lambda.$$

[22] This is in the sense that if we use vector-meson-dominance model to calculate the decay widths of $\eta \to 2\gamma$ and $\pi^0 \to 2\gamma$ by taking the V-γ couplings as defined in (IV8), we do not get the relation that $\Gamma_\eta(0,0) = (1/\sqrt{3})\Gamma_{\pi^0}(0,0)$, which is predicted by U-spin conservation.

TABLE I. Average values of a_η as function of $\Gamma_\eta(0,0)$ and $f_{\omega\pi\gamma}^2/4\pi$.

$\Gamma_\eta(0,0)$	1.38×10^{-3}				1.80×10^{-3}			
$f_{\omega\pi\gamma}^2/4\pi$	0.186α		0.14α		0.186α		0.14α	
a_η	1.45	−1.42	1.26	−1.24	1.11	−1.09	0.97	−0.93

Since the spectral function gives a very small contribution to a_η, the sign of $a_\eta = -\mathrm{sgn}(f_{\omega\pi\gamma}/[\gamma_\rho\Gamma_\eta(0,0)])$. The above expression indicates that a_η is a function of the model of $\rho(\Lambda)$, $\Gamma_\eta(0,0)$, and the vector-meson coupling constants. However, for given values of $\Gamma_\eta(0,0)$ and $f_{\omega\pi\gamma}^2/4\pi$, $|a_\eta|$ is insensitive to the other information. Table I lists the value of a_η as function of $\Gamma_\eta(0,0)$ and $f_{\omega\pi\gamma}^2/4\pi$ but averaged over the four models.

A measurement of the distribution of those lepton pairs whose three-momentum vectors make small angles, i.e., for small x, enables us to determine the sign and the magnitude of $f_{\omega\pi\gamma}/[\gamma_\rho\Gamma_\eta(0,0)]$, and hence provides us an estimate of the size of $\Gamma_\eta(0,0)$. Because a_η is not sensitive to the model of $\rho(\Lambda)$ and $f_{\omega\pi\gamma}/[\gamma_\rho g_{\rho\omega\pi}]$, no information on these aspects can be obtained.

Figures 3 to 5 show the total branching ratios of the Dalitz-pair decays and the lepton pair distributions as functions of a_η. In making these curves the full expression of $\Gamma_\eta(0,m_\eta^2 x)$ has been used. Experimentally, nothing has been known about a_η.

With appropriate changes of the vector coupling constants and the spectral function, (IV6) and (IV10) are applicable to the case of π^0. Now we have $(q-k)^2$

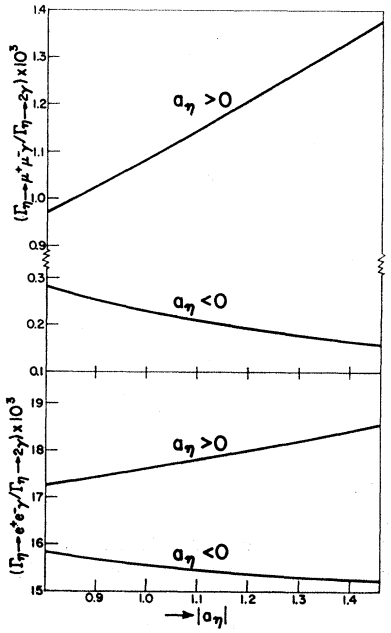

FIG. 3. Predicted branching ratio $\Gamma_\eta \to l^+l^-\gamma/\Gamma_\eta \to 2\gamma$ as a function of a_η, a parameter which is defined in the text. A measurement of the l^+l^- effective-mass distribution will give a measurement of a_η.

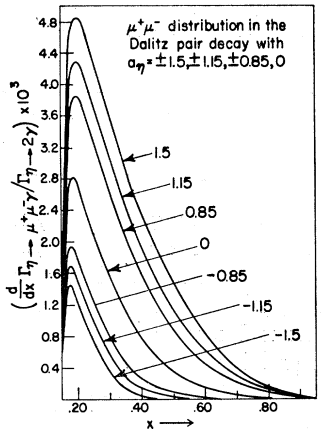

FIG. 4. Predicted μ-pair effective-mass distribution in the Dalitz-pair decay. $x=(p_1+p_2)^2/m_\eta^2$, where p_1 and p_2 are the four-momenta of the muons.

$=m_\pi^2 x$, $4m_e^2/m_\pi^2 \leqslant x \leqslant 1$. For small x, we can write

$$\Gamma_{\pi^0}(0,m_\pi^2 x)=\Gamma_{\pi^0}(0,0)(1+a_{\pi^0}x).$$

Also, the sign of $a_{\pi^0}=-\mathrm{sgn}(f_{\omega\pi\gamma}/[\gamma_\rho\Gamma_{\pi^0}(0,0)])$. Using $\Gamma_{\pi^0}(0,0)=2.4\times10^{-3}$, ($\tau_{\pi^0}\simeq1.78\times10^{-16}$ sec), and $f_{\omega\pi\gamma}^2/4\pi\simeq0.186\alpha$, for the various models and relative sign combinations, we obtain $a_{\pi^0}\simeq\pm0.06$ which is close to those obtained before.[5,21] The average experimental value of a_{π^0} is -0.25 ± 0.15,[23] which predicts that $f_{\omega\pi\gamma}/[\gamma_\rho\Gamma_{\pi^0}(0,0)]>0$. There is a discrepancy between the experimental value and the theoretically calculated one, but in view of the large experimental error, we do not yet regard this as disturbing. A more accurate measurement of a_{π^0} is clearly called for.[24]

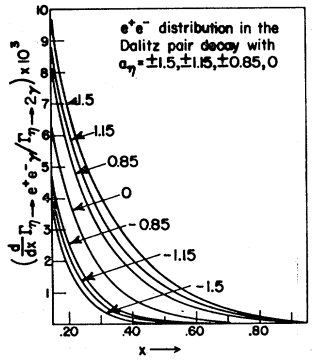

FIG. 5. Predicted e-pair effective-mass distribution in the Dalitz-pair decay. $x=(p_1+p_2)^2/m_\eta^2$, where p_1 and p_2 are the four-momenta of the positron and the electron.

[23] N. Samios, Phys. Rev. **121**, 275 (1961); H. Kobrak, Nuovo Cimento **20**, 115 (1961).

[24] In the models discussed here one may try to make up this possible disprepancy with the experimental result by choosing a model such that $H_\rho<1$. Since $|a_{\pi^0}|\sim1/H_\rho$, this increases $|a_{\pi^0}|$. This can be achieved in the dipole model; however, such a condition imposed upon $\rho(\Lambda)$ cannot satisfy the Bjorken limit. Moreover, it introduces a very strong cutoff dependence to r_D, which is hard to justify. A model like (IV16), in which there are $n-1$ free parameters, may be tried to reproduce the experimental value of a_{π^0} and at the same time to give a weak dependence of r_D on the cutoff mass.

B. Direct Decays

In order to obtain a prediction for direct decays we must evaluate the integral (II8). First we transform the integral (II8) by Feynman's technique. Then, since in all of our models of $\rho(\Lambda)$ we have $\Lambda\gtrsim\Lambda_1\gtrsim4M_N^2$ we can use $R^2=\Lambda/m_\eta^2$ as an expansion parameter to approximate integral (II8). We keep only the terms proportional to $\ln R_1^2$, constant, $\ln R_1^2/R_2^2$, and $1/R_1$ in the expansion, where $R_1^2=\Lambda_1/m_\eta^2$. The leading term in r_D is proportional to $(\ln R_1^2)^2$. The branching ratios for the e-pair process, ranging from 3×10^{-8} to 5×10^{-9},[12] are not interesting to us.

The branching ratio of the μ-pair process, which we shall denote by $r_{D\mu}$, depends more strongly on the cutoff

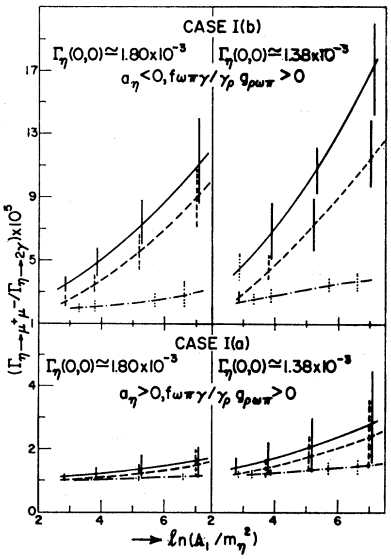

FIG. 6. Predicted branching ratio $\Gamma_{\eta\to\mu^+\mu^+}/\Gamma_{\eta\to2\gamma}$ averaged over the information of $f_{\omega\pi\gamma}^2/4\pi$ and $g_{\rho\omega\pi}^2/4\pi$. The "error bars" indicate the variation of this branching ratio under the change of $f_{\omega\pi\gamma}^2/4\pi$ and $g_{\rho\omega\pi}^2/4\pi$. The solid line is for the baryon model, the dashed line is for the δ-function model, and the dot-dashed line is for the dipole model.

mass than the corresponding cases of the e-pair process. A feature common to both the μ- and e-pair processes is that the r_D of the single-pole model in all the cases are very close to those of the δ-function model. Similarly the branching ratio of the dipole model of the two signs of $f_{\omega\pi\gamma}/[\gamma_\rho g_{NN\pi}]$ are also close to one another. The significance of this similarity of r_D in these cases will be discussed in the next section.

We plot in Figs. 6 and 7 the values of $r_{D\mu}$ obtained for the baryon model, the δ-function model, and the dipole model as a function of the various parameters. Figure 6 shows the values of $r_{D\mu}$ for $f_{\omega\pi\gamma}/[\gamma_\rho g_{\rho\omega\pi}]>0$. For a given value of $\Gamma_\eta(0,0)$ and given sign of a_η, we average over the information of $f_{\omega\pi\gamma}$ and $g_{\rho\omega\pi}$. The "error bars" associated with each curve represent the variation of $r_{D\mu}$ as the values of $f_{\omega\pi\gamma}$ and $g_{\rho\omega\pi}$ are changed. The upper ends of the "error bars" are at those

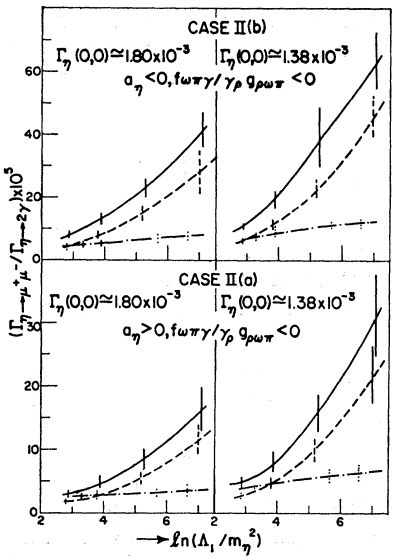

FIG. 7. Predicted branching ratio $\Gamma_{\eta\to\mu^+\mu^-}/\Gamma_{\eta\to2\gamma}$. See explanation under Fig. 6.

$r_{D\mu}$ for which $f_{\omega\pi\gamma}^2/4\pi\simeq0.186\alpha$, $g_{\rho\omega\pi}^2/4\pi\simeq0.3$, and the lower ends of the "error bars" are at $f_{\omega\pi\gamma}^2/4\pi\simeq0.14\alpha$, $g_{\rho\omega\pi}/4\pi\simeq0.5$. Similarly in Fig. 7 we plot $r_{D\mu}$ for $f_{\omega\pi\gamma}/[\gamma_\rho g_{\rho\omega\pi}]<0$. In this graph the upper ends of the "error bars" are at those $r_{D\mu}$ for which $f_{\omega\pi\gamma}^2/4\pi\simeq0.186\alpha$, $g_{\rho\omega\pi}/4\pi\simeq0.5$, and the lower ends of the "error bars" are at $f_{\omega\pi\gamma}^2/4\pi\simeq0.14\alpha$, $g_{\rho\omega\pi}^2/4\pi\simeq0.3$.

It can be shown that[2,3,12]

$$\mathrm{Im}\{3A+(1-4\xi_l^2)B\}=(\pi/2)(1-4\xi_l^2)\ln\xi_l^2-12\xi_l^2.$$

This is independent of the model of strong interactions at the $\eta\gamma\gamma$ vertex; therefore we can set a lower bound for the direct branching ratios:

$$r_D\gtrsim 2\left(\frac{\alpha}{\pi}\right)^2(1-4\xi_l^2)(\pi\ln\xi_l)^2$$

then

$$r_D\gtrsim 10^{-5},\quad \text{for the } \mu\text{-pair process}$$
$$r_D\gtrsim 10^{-9}\quad \text{for the } e\text{-pair process}.$$

Since the leading term in r_D is proportional to $(\ln R_1^2)^2$, one may expect a strong dependence of $r_{D\mu}$ on the cutoff mass Λ_1. This is true for some of the sign combinations of a_η and $f_{\omega\pi\gamma}/[\gamma_\rho g_{\rho\omega\pi}]$. But $r_{D\mu}$ is rather insensitive to Λ for some other sign combinations, as can be readily seen from Figs. 6 and 7.

VI. DISCUSSION

We shall discuss first what information we can obtain about the high-energy behavior of $\Gamma_\eta(k_1^2,k_2^2)$ from the direct-decay branching ratios calculated in the last section (Figs. 6 and 7). Second, we shall discuss what can test the models presented in this paper. We shall restrict ourselves to the μ-pair process. Its branching ratio will be denoted as $r_{D\mu}$.

We separate $r_{D\mu}$ according to the signs of a_η and $f_{\omega\pi\gamma}/[\gamma_\rho g_{\rho\omega\pi}]$ (see Figs. 6 and 7). Since all four models give approximately the same magnitude of a_η for a given sign of a_η, they all have the same low-energy behavior as expected. An examination of Figs. 6 and 7 shows that the high-energy behavior of the form factor is different in each of the four models, except that the δ-function and the single-pole models give similar results. Also, the form factor depends on the sign of a_η and $f_{\omega\pi\gamma}/[\gamma_\rho g_{\rho\omega\pi}]$. Therefore an understanding of the structure of $\Gamma_\eta(k_1^2,k_2^2)$ in terms of our models depends on resolving the sign ambiguities of a_η and $f_{\omega\pi\gamma}/[\gamma_\rho g_{\rho\omega\pi}]$ as well as their magnitude.

Presently both signs can be determined by means of theoretical models. The sign of a_η is predicted to be negative if we accept the validity of U-spin conservation, and assume that the experimental measurement of the sign of a_{π^0} is correct. (The experiment says that a_{π^0} is negative,[23] but the error is large enough so that the result is not conclusive.) The sign of $f_{\omega\pi\gamma}/[\gamma_\rho g_{\rho\omega\pi}]$ is positive if we use the vector-meson-dominance model to relate the $\omega\pi\gamma$ coupling to the $\rho\omega\pi$ coupling through the ρ-γ transition, i.e., $f_{\omega\pi\gamma}/[\gamma_\rho g_{\rho\omega\pi}]=e/\gamma_\rho^2>0$.

However there are reasons that these predictions have to be checked experimentally. For instance, both the too-small theoretical prediction of a_{π^0} and the too-large theoretical prediction of $\Gamma_{\pi^0}(0,0)$ by the vector-meson-dominance model raise doubts as to the validity of this simple model and makes the conclusion that $a_\eta<0$ questionable. Also in a gauge-invariant theory of the V-γ coupling, $f_{\omega\pi\gamma}$ and $g_{\rho\omega\gamma}$ may not be related at all. For example, in the present work $f_{\omega\pi\gamma}$ is the subtracted term of the $\omega\pi\gamma$ vertex function, chosen to be the phenomenological coupling constant of the $\omega\pi\gamma$ interaction (all the particles are on the mass shell), whereas $g_{\rho\omega\pi}$ occurs in the coefficient of the ρ-meson pole contribution. Hence $f_{\omega\pi\gamma}$ and $g_{\rho\omega\pi}$ are independent.

From Sec. V and Figs. 6 and 7, we can make the following observations:

(1) The decay branching ratios $r_{D\mu}$ in Fig. 6 ($f_{\omega\pi\gamma}/[\gamma_\rho g_{\rho\pi\omega}]>0$) are less sensitive to the cutoff masses than those in Fig. 7 ($f_{\omega\pi\gamma}/[\gamma_\rho g_{\rho\omega\pi}]<0$). Hence the high-energy behavior is less crucial in the former cases than in those of the later cases.

(2) In case I(a) of Fig. 6, $r_{D\mu}$ is surprisingly insensitive to the cutoff mass for all the models. This is the case that $f_{\omega\pi\gamma}/[\gamma_\rho g_{\rho\omega\pi}]>0$ and $a_\eta>0$ [$f_{\omega\pi\gamma}/(\gamma_\rho g_{\rho\omega\pi})<0$]. The other extreme happens in case II(b), Fig. 7, for which $f_{\omega\pi\gamma}/[\gamma_\rho g_{\rho\omega\pi}]<0$ and $a_\eta<0$.

(3) The spectral functions of the single-pole model and the δ-function model have the same threshold behavior. They possess, however, different asymptotic behavior, going like $1/k_0^2$ and $1/k_0^4$, respectively. The approximate equality of $r_{D\mu}$ for all the cases in these two models (as mentioned in the last section) indicates that the asymptotic behavior is not crucial, at least in these two models.

(4) The relative sign of $f_{\omega\pi\gamma}/\gamma_\rho$ and the Bjorken limit (i.e., the sign of $f_{\omega\pi\gamma}/[\gamma_\rho g_{NN\pi}]$) is not important. This is indicated by the fact that in the dipole model both signs of $f_{\omega\pi\gamma}/[\gamma_\rho g_{NN\pi}]$ give almost identical $r_{D\mu}$, as has been mentioned in Sec. V.

(5) The imposition of the Bjorken limit reduces, in general, both the values of $r_{D\mu}$ and the overlapping between the various cases of $r_{D\mu}$.

A. Test of the Theoretical Models

As one may expect, a test of the theoretical models constructed in the present work needs detailed experimental information. At the present time only $f_{\omega\pi\gamma}^2/4\pi$, $\Gamma_{\pi^0}(0,0)$, and $\gamma_\rho^2/4\pi$ are reliably measured to some extent. Other experimental data, e.g., $f_{\omega\pi\gamma}/[\gamma_\rho g_{\rho\omega\pi}]$, a_η, etc., either do not exist or possess such great uncertainties that they are essentially open questions. In the following we shall point out the experiments that are expected to be carried out and the information that is obtainable from them. Before going on we should like to mention that since $r_{D\mu}\gtrsim 10^{-5}$, the direct decays can be easily distinguished from the background contribution of the Dalitz-pair decays occurring with soft-photon emission.

(a) Measurements of a_η and a_{π^0} and the Test of $SU(3)$

The measurements of a_η and a_{π^0} will not only separate case I(a) from case I(b), and case II(a) from II(b), but also test $SU(3)$ invariance and the ω-φ mixing theory (see Figs. 6 and 7).

(b) Measurement of $f_{\omega\pi\gamma}/[\gamma_\rho g_{\rho\omega\pi}]$

A measurement of the sign of $f_{\omega\pi\gamma}/[\gamma_\rho g_{\rho\omega\pi}]$ will distinguish between Figs. 6 and 7, and together with the information of (a), will determine which case applies. As $f_{\omega\pi\gamma}^2/4\pi$ and $\gamma_\rho^2/4\pi$ are known, this also provides an estimate of $g_{\rho\omega\pi}^2/4\pi$. Then a prediction of the magnitude of $r_{D\mu}$ can be made. However, it is doubtful that the measurement of the sign of $f_{\omega\pi\gamma}/[\gamma_\rho g_{\rho\omega\pi}]$ can be carried out in the near future. Hence one can only check the consistency of $r_{D\mu}$ with some choice of this sign. Again theory expects the sign to be positive.

(c) Test of the High-Energy Behavior of $\Gamma_\eta(k_1^2,k_2^2)$

If the above information becomes available, we may determine the high-energy behavior of $\Gamma_\eta(k_1^2,k_2^2)$ in terms of the models we have constructed. In addition, if we know the values of $r_{D\mu}$, then, by restricting ourselves to a certain model of the spectral function (e.g., the dipole model), we can determine the cutoff mass. Therefore both the low-energy and the high-energy functions of $\Gamma_\eta(k_1^2,k_2^2)$ are determined.

(d) Test of the Asymptotic Behavior of $\Gamma_\eta(k_1^2,k_2^2)$ and the Bjorken Limit

The $1/k_0^2$ behavior of $\Gamma_\eta(k^2, (q-k)^2)$ is hard to test. The observation (c) seems to suggest that we have to take this behavior as an assumption, or at least what has been considered in the present work does not provide a way to check this asymptotic behavior.

The consistency of the assumption of the Bjorken limit can be checked only in a very special situation and with a special model of the spectral function. To illustrate this, let us consider the following example. Suppose that the spectral function can be described by either the baryon model which does not satisfy the Bjorken limit or the dipole model which satisfies the Bjorken limit. Then a test of the plausibility of the Bjorken limit is to find out which model is suitable. This is possible only when we know the signs of a_η and $f_{\omega\pi\gamma}/[\gamma_\rho g_{\rho\omega\pi}]$, and the values of $\Gamma_\eta(0,0)$, $f_{\omega\pi\gamma}^2/4\pi$, and $g_{\rho\omega\pi}^2/4\pi$. In addition we have to assume that the $SU(3)$ assumption in deriving the low-energy function L is correct. For example, suppose we know $r_{D\mu}$ is in case I(b) and $\Gamma_\eta(0,0)\simeq 1.8\times 10^{-3}$, $f_{\omega\pi\gamma}^2/4\pi\simeq 0.186\alpha$, $g_{\rho\omega\pi}^2/4\pi \simeq 0.3$. Then if $r_{D\mu}\simeq 3.5\times 10^{-5}$ we know that the dipole model is more reasonable, and this makes it plausible that the Bjorken limit is satisfied. Otherwise, no conclusion can be made. This test is not likely to be performed in the near future.

B. Predictions of the Models

Because we are lacking most of the experimental information, we should like to ask what the models can predict, and what are the minimum amount of experimental data required in this connection. To answer this question, we want to show in the following example that if we know a_η and $r_{D\mu}$, a number of predictions can be made. Among the various experiments needed to be performed, experiments to obtain a_η and $r_{D\mu}$ are most likely to be carried out.

To be specific, let us take the dipole model as an example. Suppose that a measurement of a_η gives the result, for instance, $a_\eta\simeq+1.2$, then we may conclude that we are in case I(a) (see Fig. 6) or case II(a) (see Fig. 7). In addition, we can infer from Table I that the information of $\Gamma_\eta(0,0)$ and $f_{\omega\pi\gamma}^2/4\pi$ are either $\Gamma_\eta(0,0) \simeq 1.8\times 10^{-3}$ and $f_{\omega\pi\gamma}^2/4\pi\simeq 0.186\alpha$, or $\Gamma_\eta(0,0)\simeq 1.38 \times 10^{-3}$ and $f_{\omega\pi\gamma}^2/4\pi\simeq 0.14\alpha$. Hence if further we know the value of $\Gamma_\eta(0,0)$, we know $f_{\omega\pi\gamma}^2/4\pi$ or vice versa. Therefore this enables us to get more information about the vector coupling. If a measurement of $r_{D\mu}$ gives the result that $r_{D\mu}\simeq 1.5\times 10^{-5}$ we see that we are in case I(a) or I(b) (see Fig. 6), or more specificially, in case I(a) which implies $f_{\omega\pi\gamma}/[\gamma_\rho g_{\rho\omega\pi}]>0$. However, it does not predict the magnitude of $g_{\rho\omega\pi}^2/4\pi$ (nor the sign of $f_{\omega\pi\gamma}/[\gamma_\rho g_{NN\pi}]$). If $r_{D\mu}\gtrsim 3\times 10^{-5}$ then we are in case II(a) and the sign of $f_{\omega\pi\gamma}/[\gamma_\rho g_{\rho\omega\pi}]$ is negative.

On the other hand, if a measurement of a_η is, for example, -1.4, then $f_{\omega\pi\gamma}/[\gamma_\rho\Gamma_\eta(0,0)]>0$. From Table I we obtain $\Gamma_\eta(0,0)\simeq 1.38\times 10^{-3}$ and $f_{\omega\pi\gamma}^2/4\pi\simeq 0.186\alpha$. If a measurement of $r_{D\mu}$ has the value 4×10^{-5} or less, then we are in case I(b) (see Fig. 6). If a measurement of $r_{D\mu}$ has the value 10^{-4} or more, we are in case II(b).

If in particular the value of $r_{D\mu}$ falls between 4×10^{-5} and 10^{-4}, it can be explained by a higher cutoff mass of Λ_1 in case I(b).

Similar discussions can be given to other models. Nevertheless, the situation is more complicated because of the overlapping between the various cases. Definite prediction by measuring a_η and $r_{D\mu}$ is not feasible unless we can nail down the values of $\Gamma_\eta(0,0)$, $f_{\omega\pi\gamma}^2/4\pi$, and $g_{\rho\omega\pi}^2/4\pi$.

The above examples show very positive predictions. However, this needs very accurate measurement of $r_{D\mu}$, which is rather difficult.

To end our discussion we make the following remarks:

(a) If $r_{D\mu}\simeq10^{-5}$, i.e., its minimum value, the imaginary part dominates the decay amplitude. Unless the very unlikely situation occurs in which the virtual photons always stay approximately on their mass shell, there are high-mass intermediate states operating at the $\eta\gamma\gamma$ vertex, and their contributions to the real part must cancel each other. Our models indicate that case I(a) has to be taken.

(b) If $r_{D\mu}\simeq10^{-4}$, which indicates a rather large value, we can hardly draw a useful conclusion unless more accurate information about the vector couplings is given. This indicates also that we have to probe a high value of the cutoff mass Λ_1.

(c) There are other possible models that have not been considered in this work. For example, we can take the following form for $\Gamma_\eta(k_1^2,k_2^2)$:

$$\Gamma_\eta(k_1^2,k_2^2)=\sum_{V_1,V_2}\frac{\lambda_{V1}\lambda_{V2}g_{V1V2}}{(m_{V_1}^2-k_1^2)(m_{V_2}^2-k_2^2)}+B(k_1^2,k_2^2).$$

The first term on the right-hand side of the above expression comes from the vector-meson contributions. The second term represents all the high-mass contributions. If again we take

$$B(k_1^2,k_2^2)=\int d\Lambda\,\rho(\Lambda)\Lambda^2/[(\Lambda-k_1^2)(\Lambda-k_2^2)],$$

under certain conditions on the vector couplings this form can be reduced to what we have constructed. If we also take

$$\rho(\Lambda)=\textstyle\sum_i(\beta_i\Lambda_i/\Lambda^2)\theta(\Lambda-\Lambda_i),$$

then

$$\textstyle\sum_i\beta_i\Lambda_i/m_\eta^2=C_{\rm BL}.$$

Because of the smallness of the Bjorken limit, as before the high-energy function will not make a very important contribution to the branching ratio $r_{D\mu}$.

In summary, we may conclude that the vector mesons play an important role in the direct-decay process $\eta\to\mu^+\mu^-$. Therefore a measurement of the branching ratio $r_{D\mu}$ for this process would not provide at present an unambiguous determination of the high-mass properties of the $\eta\gamma\gamma$ form factor. This, however, does not make the value of $r_{D\mu}$ uninteresting, especially in the case of large $r_{D\mu}$, i.e. $r_{D\mu}\gtrsim10^{-4}$.[25] In this eventuality its full usefulness will require more extensive experiments on the other decay modes of η and π^0. Once the unknown parameters such as $\Gamma_\eta(0,0)$, a_{π^0}, a_η, etc., are well determined and the validity of $SU(3)$ invariance on the vector couplings checked, a more detailed analysis of the model dependence of the theory should be undertaken.

ACKNOWLEDGMENTS

The author is deeply grateful to Professor D. A. Geffen for suggesting this problem and for his constant guidance throughout this work. Special thanks are due Professor H. Suura for valuable discussions. The author very helpful suggestions and comments and Dr. D. G. Sutherland for comments.

APPENDIX A

Following Ref. 7 we shall assume that the matrix element of (II4) can be truncated and that the commutator of the two components of the electromagnetic current can be evaluated in the quark model. Then we have

$$\Gamma_{\mu\nu}(k,q-k)\xrightarrow[|k_0|\to\infty,\mathbf{k}\text{ finite}]{}-\frac{1}{k_0}\int d^3x\,e^{-i\mathbf{k}\cdot\mathbf{x}}\times\langle0|[J_\mu(0,\mathbf{x}),J_\nu(0)]|q\rangle+O(1/k_0^2).$$

Using a quark structure for the electromagnetic current $J_\mu=\bar\psi\gamma_\mu Q\psi$, where ψ is the quark field, and $Q=T_3+\frac{1}{2}Y$, we get

$$[J_\mu(0,\mathbf{x}),J_\nu(0)]=-2ie^2\varepsilon_{\mu\nu\lambda\tau}\zeta^\lambda j_5^\tau(0)\delta(\mathbf{x})+\text{grad. term},$$

where $\zeta=(1,0,0,0)$, $\varepsilon_{\mu\nu\lambda\tau}$ is the complete antisymmetric tensor of the Minkowski space $\varepsilon_{0123}=1$, and the gradient term is the so-called Schwinger term which will be ignored here.[7] The current f_5^σ is defined by

$$j_5^\sigma=(2/9)\bar\psi\gamma_5\gamma^\sigma\psi+(1/3)\bar\psi\gamma_5\gamma^\sigma Q\psi.$$

The expression for Q enables us to write

$$j_5^\sigma=(2/9)A_\sigma^{X^0}+(1/3)A_\sigma^{\pi^0}+(1/3\sqrt3)A_\sigma^\eta,$$

where A^i, $i=X^0$, π^0, η, are the axial vector currents which transform under $SU(3)$ like the particle i. Now we may write

$$\Gamma_{\mu\nu}(k,q-k)\xrightarrow[|k_0|\to\infty]{}(2ie^2/k_0^2)\varepsilon_{\mu\nu\lambda\tau}(k_0\zeta)^\lambda\times\langle0|j_5^\tau|q\rangle+O(1/k_0^2).$$

By $SU(3)$ invariance, it is clear that only the term A_σ^η in $j_{5\sigma}$ contributes if the mixing effect between X^0 and η is negligible.[26] By PCAC and in the limit of

[25] In this circumstance, case I(a) of Fig. 6 will be excluded. If $a_\eta>0$ this would require a large value of Λ.

[26] The X^0-η mixing angle is small. General theoretical estimations are about 10° (D. A. Geffen, private communication). Because of the uncertainties in the vector coupling constants and the error in identifying $C_\eta=C_{\pi^0}$ in using exact $SU(3)$ symmetry, the omission of the X^0-η mixing is reasonable.

exact symmetry,

$$\langle 0|A_\sigma{}^\eta|q\rangle = iC_{\pi^0}q_\sigma,$$

where $C_{\pi^0}=M_N F_A/g_{NN\pi}$, $F_A=1.18$, $g_{NN\pi}{}^2/4\pi\simeq 14.6$. We get therefore

$$\Gamma_{\mu\nu}(k, q-k) \xrightarrow[|k_0|\to\infty]{} -(e^2/k_0{}^2)\varepsilon_{\mu\nu\lambda\tau}(k_0\zeta)^\lambda \times q^\tau(2C_{\pi^0}/3\sqrt{3})+O(1/k_0{}^2).$$

Keeping only the leading term of the $1/k_0$ expansion in $\Gamma_{\mu\nu}$, we obtain (II3).

APPENDIX B

We want to show that the asymptotic condition (IV8) and the normalization condition (IV11) imply that

$$\lim_{\Lambda\to\infty}\rho(\Lambda)\to \text{const}/\Lambda^2.$$

Before going on, we state the following two restrictions on the spectral function, which are easy to prove:

(a) The normalization condition requires that $\rho(\Lambda)$ has to decrease faster than $1/\Lambda$. This can be proved from the normalization condition.

(b) The spectral function $\rho(\Lambda)$ must decrease no faster than $1/\Lambda^3$. Otherwise $\int d\Lambda\,\Lambda^2\rho(\Lambda)$ converges and it is easy to show that $\lim_{|k_0|\to\infty}H(k^2, (q-k)^2)\sim 1/k_0{}^4$ which contradicts the asymptotic condition (IV8). It can also be shown that if $\rho(\Lambda)\to 1/\Lambda^3$, the asymptotic condition is also violated.

We must have

$$\rho(\Lambda)\to C_0/\Lambda^\lambda,$$

where $1<\lambda<3$. We want to show that $\lambda=2$.

Suppose $1<\lambda<2$. Let us consider an auxiliary function

$$f_1(z)=f(0)+\frac{z}{\pi}\int_{\Lambda_1}^{\infty} dx\, x^2\rho(x)/[x(x-z)],$$

then

$$H(k, (q-k)^2) \xrightarrow[|k_0|\to\infty]{} \frac{1}{2q_0k_0}\lim_{|k_0|\to\infty}\{f_1(k^2)-f_1((q-k)^2)\}.$$

Hence we need

$$\lim_{|k_0|\to\infty}[f_1(k^2)-f_1((q-k)^2)]\to \text{const}/k_0. \quad \text{(B1)}$$

When z is very large we can use the asymptotic form of $\rho(\Lambda)$:

$$f_1(z)\simeq f_1(0)+\frac{z}{\pi}\int_{\Lambda_1}^{\infty}\frac{dx\, x^2(C_0/x^\lambda)}{[x(x-z)]} = f_1'(0)+\frac{C_0 z}{\pi}\int_0^\infty \frac{dx}{[x^{\lambda-1}(x-z)]},$$

where $f_1'(0)$ is another constant. In the above expression we have extended the lower limit of integration from Λ_1 to 0. The extra contribution to the integral from 0 to Λ_1 is taken care of by changing $f_1(0)$ to $f_1'(0)$. The integrand has a singularity at $x=0$; since $\lambda-1<1$, this singularity does not cause trouble.

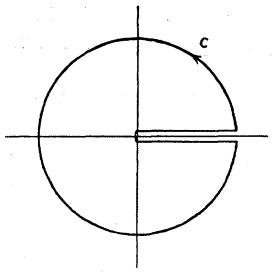

FIG. 8. The contour of integration of (B2).

Let us consider the following function:

$$\varphi(z)=1/z^{\lambda-1}.$$

By Cauchy's integral formula, we have

$$\varphi(z)=\frac{1}{2\pi i}\int_C \frac{dx\,\varphi(x)}{(x-z)}, \quad \text{(B2)}$$

where C is the contour shown in Fig. 8. Since $0<\lambda-1<1$, we can write

$$\varphi(z)=\frac{1}{2\pi i}\int_{0+i\epsilon}^{\infty+i\epsilon}\frac{dx\,\varphi(x)}{(x-z)}+\frac{1}{2\pi i}\int_{\infty-i\epsilon}^{0-i\epsilon}\frac{dx\,\varphi(x)}{(x-z)} =\frac{1}{2\pi i}\int_0^\infty \frac{dx\,(1/x^{\lambda-1}-e^{-2\pi i(\lambda-1)}/x^{\lambda-1})}{(x-z)}.$$

We obtain therefore

$$\int_0^\infty \frac{dx}{[x^{\lambda-1}(x-z)]}=\frac{[\pi e^{i\pi(\lambda-1)}/\sin(\lambda-1)\pi]}{z^{\lambda-1}}.$$

Then we obtain

$$f_1(z)=f_1'(0)+\frac{C_0\pi e^{i\pi(\lambda-1)}}{\sin(\lambda-1)\pi}\frac{1}{z^{\lambda-1}},$$

$$f_1(k^2)-f_1((q-k)^2)\xrightarrow[|k_0|\to\infty]{} -\frac{C_0\pi e^{i\pi(\lambda-1)}}{\sin(\lambda-1)\pi}\frac{2(\lambda-1)q_0}{k_0{}^{2\lambda-1}},$$

which contradicts the asymptotic condition (B1).

For $2<\lambda<3$, we can consider another auxiliary function

$$f_2(z)=\int_{\Lambda_1}^\infty \frac{dx\, x^2\rho(x)}{(x-z)}.$$

By a similar procedure we can show that the asymptotic condition (IV8) cannot be satisfied either.

It is now an easy matter to check that for $\lambda=2$ the high-energy function does satisfy the asymptotic condition (IV8).